

**BACK EMF CALCULATIONS FOR
AXIAL-GAP PERMANENT MAGNET SYNCHRONOUS MOTORS (AGPMSM)
WITH DISC MAGNETS***

J. M. Bailey¹, B. Ozpineci¹, G. W. Ott¹, and D. S. Daniel²

¹Oak Ridge National Laboratory
Oak Ridge, Tennessee

²The University of North Florida
Jacksonville, Florida

* Prepared by Oak Ridge National Laboratory, managed by UT-Battelle, LLC, for the U.S. Department of Energy under contract DE-AC05-00OR22725.

The submitted manuscript has been authored by a contractor of the U.S. Government under contract DE-AC05-00OR22725. Accordingly, the U.S. Government retains a nonexclusive, royalty-free license to publish or reproduce the published form of this contribution, or allow others to do so, for U.S. Government purposes.

BACK EMF CALCULATIONS FOR AXIAL-GAP PERMANENT MAGNET SYNCHRONOUS MOTORS (AGPMSM) WITH DISC MAGNETS

INTRODUCTION

Permanent magnet (PM) electrically commutated rotating machines can be characterized as radial-gap or axial-gap configurations. In the radial-gap configuration, the stator is in the form of a cylinder with the electrical coils in slots with coil currents in the axial or z direction. The magnets are polarized in the radial or r direction. In the axial-gap configuration, the stator is in the form of a toroid with electrical coils in slots with coil current in the radial or r -direction. The magnets, mounted on the rotor, are polarized in the axial or z -direction. In both configurations, the torque is in the angular or theta direction. The axial-gap motor has several advantages over the radial-gap motor [1,2] and has been presented as a viable candidate for the electric or hybrid electric car [3,4,5]. As the technology improves, the speed requirements are now in the 10,000-rpm range [6]. At these speeds, the axial-gap configuration has a significant advantage over the radial-gap configuration in that the magnetic containment systems do not encroach on the very valuable air-gap volume.

Oak Ridge National Laboratory (ORNL) has developed several high-speed axial-gap permanent magnet synchronous motors (AGPMSM) suitable for high-speed traction applications where the magnets are in the shape of a disc and the stator windings are sinusoidally distributed. The magnets are inserted in a nonmagnetic cartridge and then positioned on a flat plate of magnetic steel, which serves as the return path for the magnets. The containment system then consists of a ring of maraging steel. Figure 1 is a sketch of a typical system. Figure 2 shows an eight-pole cartridge with the containment ring. There is another version of ORNL's AGPMSM that uses two stators and the rotor is between the two. This version was used to drive a flywheel.

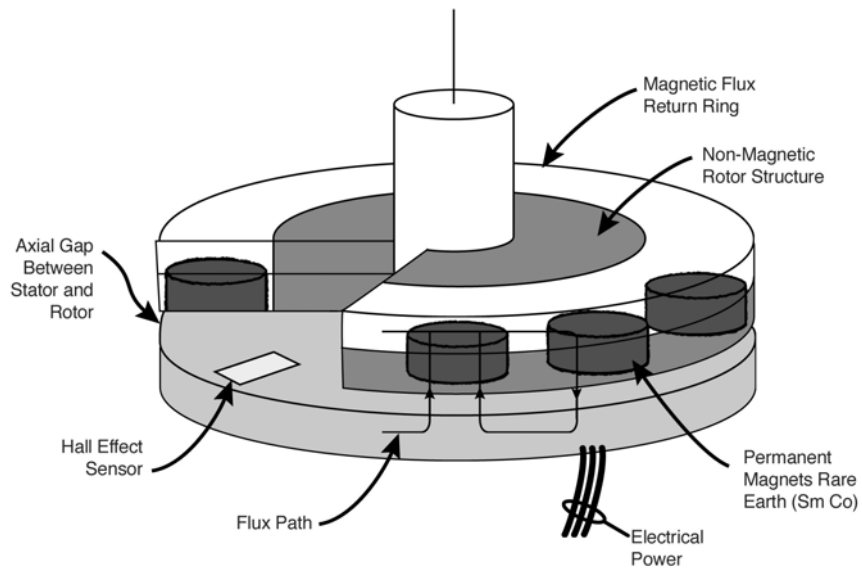


Fig. 1. Schematic of a typical AGPMSM.

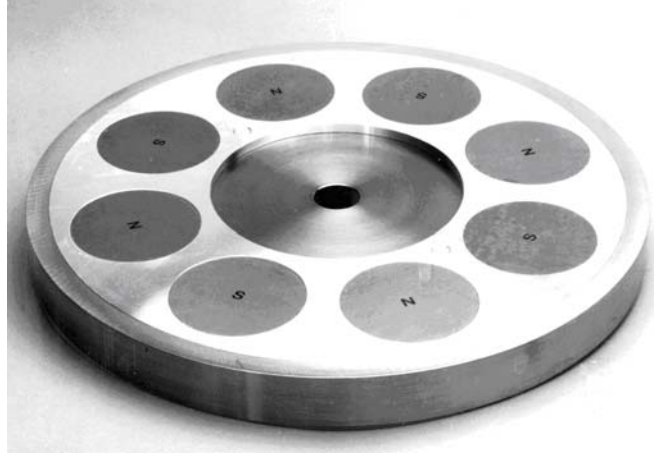


Fig. 2. An eight-pole rotor.

The success of this configuration depends upon the fidelity of the back emf compared to a true sine wave voltage. This paper develops the equations for the back emf of an AGPMSM and compares it to a true sine wave. With the proper choice of variables, the equations will apply to either the single or double stator configuration. In the following derivations; however, we will model the single stator AGPMSM.

EXPERIMENTAL TEST MOTOR

The test motor is a 3-phase, 8-pole motor with 48 slots. Each stator pole consists of six slots. Thus, there are two slots per pole per phase. This is a double layer winding in that one side of coil 1 is in the top of slot 1 and the other side is in the bottom of slot 6 (we have short chorded the coils by one slot). The two sides of coil 2 follow the same pattern; i.e., slots 2 and 7. The voltages induced in these conductors add as vectors. Each phase consists of eight such groups. The motor parameters are shown in Table 1.

Table 1. Experimental test motor parameters

PARAMETERS	SYMBOL	VALUE
# Coils	N_c	48
Turns/Coil	N_t	2
# Slots	N_{sl}	48
Poles	P	8
Outer radius	r_o	7.62 cm
Inner radius	r_i	4.45 cm
Magnet radius	R_M	0.79 cm

THE COORDINATE SYSTEM

As one conductor sweeps over a magnet, there will be an induced voltage V_c given by Eq. (1)

$$V_c = B_{ag} \cdot L \cdot R \cdot \omega, \quad (1)$$

where

- B_{ag} = Airgap flux density in Wb/sq. meters,
- L = Conductor length in meters,
- R = Radius arm in meters, and
- ω = Speed in rad/sec.

To relate the dimensions of the test motor to Eq. (1), we make use of the cylindrical coordinate system shown in Fig. 3. Any point on the circumference of the magnet (r_1 , r_2) can be found utilizing the law of cosines, i.e.

$$R_m^2 = R^2 + r^2 - 2 \cdot r \cdot R \cdot \cos(\gamma). \quad (2)$$

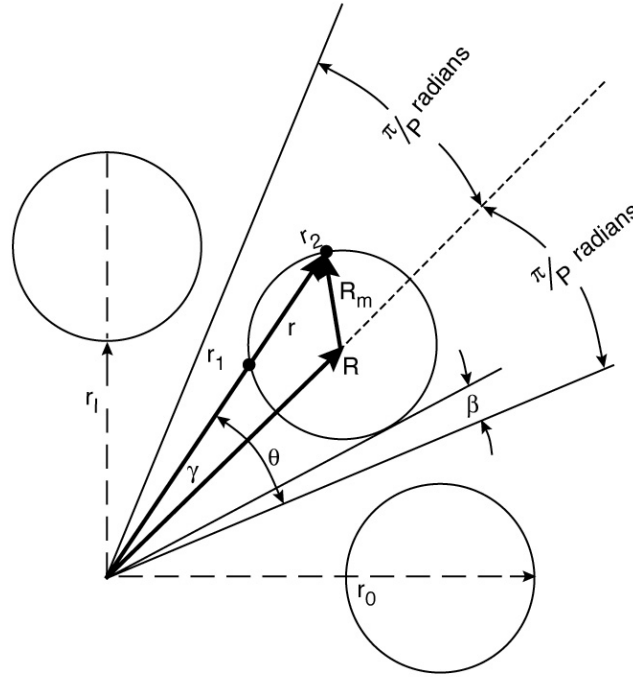


Fig. 3. The coordinate system.

We note that

$$\gamma = \theta - \frac{\pi}{P} = \theta - \frac{\pi}{8}, \quad (3)$$

$$R_m = (r_o - r_i) / 2, \quad (4)$$

$$R = r_i + R_m. \quad (5)$$

Substituting Eqs. (3), (4), and (5) into Eq. (2) we obtain the second order equation in the variable r ;

$$r^2 - r \cdot (r_i + r_o) \cdot \cos\left(\frac{\pi}{8} - \theta\right) + r_i \cdot r_o = 0. \quad (6)$$

The solution to Eq. (6) defines the two points (r_1 , r_2) on the circumference of the magnet. Thus

$$r_2 = a + b, \quad (7)$$

$$r_1 = a - b, \quad (8)$$

where

$$a = (r_o + r_i) \cdot \cos\left(\frac{\pi}{8} - \theta\right) / 2, \quad (9)$$

and

$$b = \text{sqr}t\left[\left(r_o + r_i\right)^2 \cdot \cos^2\left(\frac{\pi}{8} - \theta\right) / 4 - r_o \cdot r_i\right]. \quad (10)$$

The length of the conductor as it sweeps across the magnet varies with θ . This length L is the difference between r_2 and r_1 , i.e.

$$L = r_2 - r_1 = (a + b) - (a - b) = 2b. \quad (11)$$

To properly account for the length and radius arm of the conductor, we make use of an infinitesimal length dr on the conductor.

Equation (1) now becomes

$$V_c = B_{ag} \cdot \omega \cdot \int_{r_i}^{r_o} r dr. \quad (12)$$

Performing the integral in Eq. (12)

$$V_c = B_{ag} \cdot \omega \cdot (r_2^2 - r_1^2) / 2. \quad (13)$$

Making use of Eqs. (7) and (8) we obtain

$$r_2^2 - r_1^2 = (a + b)^2 - (a - b)^2 = 4ab. \quad (14)$$

We now have the voltage induced in one conductor as it sweeps across the magnet

$$V_c = 2 \cdot a \cdot b \cdot B_{ag} \cdot \omega. \quad (15)$$

Remembering that the 48 slots are spaced 7.5° apart, we can now construct a diagram of the flattened stator for one group as shown in Fig. 4.

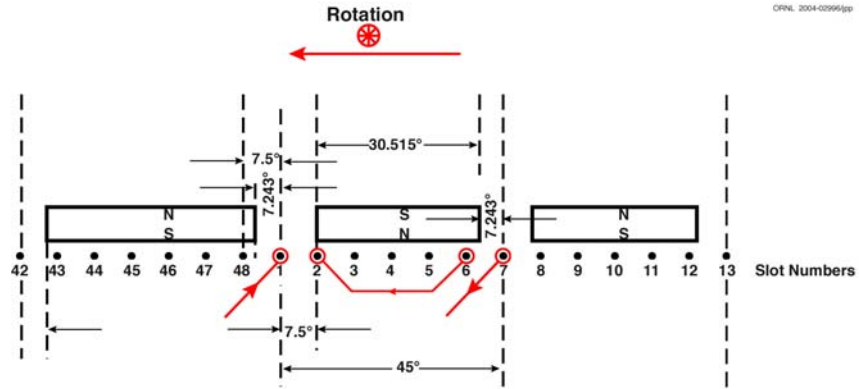


Fig. 4. Flattened diagram for three poles.

Figure 5 shows the back emf waveform calculated by inserting the machine parameters in Table 1 in Eq. (15). The effects of the magnets on the back-emf voltage can be observed from this waveform. The measured back emf waveform is shown in Fig. 6. To validate Eq. (15), the waveform in Fig. 5 is overlapped on the measured back emf waveform in Fig. 6. The comparison shows a close match.

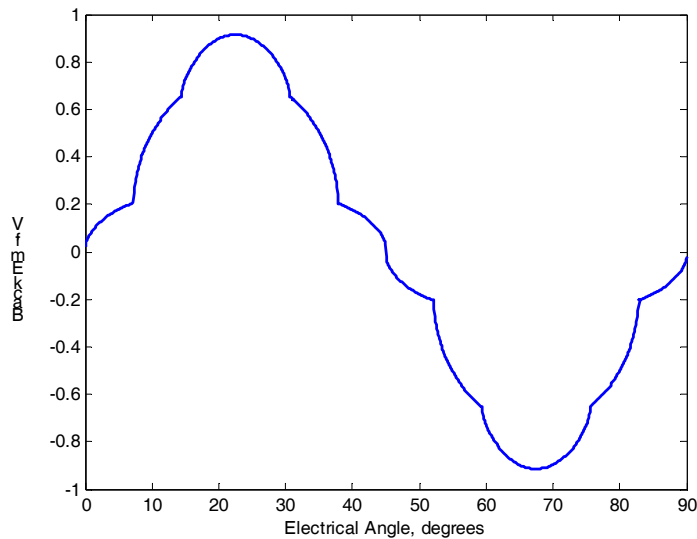


Fig. 5. Back emf at 973 rpm.

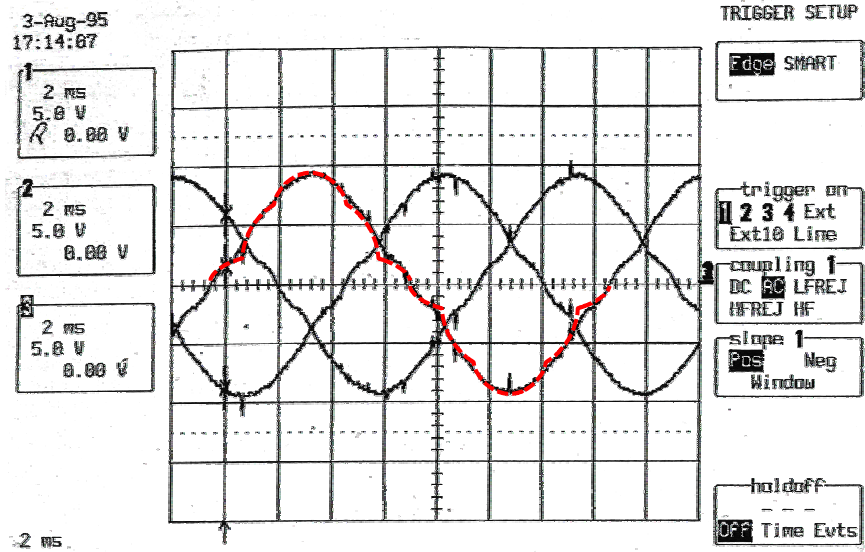


Fig. 6. Experimental and calculated back emf waveforms at 973 rpm.

CONCLUSIONS

The correlation between the calculated and the measured values show that Eq. (15) is an excellent characterization of the AGPMSM with disc magnets. With its rugged construction, AGPMSM is a viable candidate for an electric or hybrid electric vehicle traction drive. The final paper will include more experimental results with dynamic simulation of the motor.

REFERENCES

1. K. Sitapati and R. Krishnan, "Performance Comparisons of Radial and Axial Field, Permanent-Magnet, Brushless Machines," *IEEE Transactions on Industry Applications*, **37**, No. 5, September/October 2001.
2. Z. Zhang, F. Profumo, and A. Tenconi, "Axial Flux versus Radial Flux PM Motors," pp. A4-19 in *Conference Records of Speedam '96*, Capri, Italy, 1996.
3. F. Profumo, Z. Zhang, and A. Tenconi, "Axial Flux Machines Drivers: A New Viable Solution for Electric Cars," pp. 39-45 in *IEEE Transactions on Industrial Electronics*, **44**, No. 1, February 1997.
4. J. F. Eastham, M. J. Balchin, T. Betzer, H. C. Lai, and S. Gair, "Disc Motor with Reduced Unsprung Mass for Direct EV Wheel Drive," pp. 569-573 in *Proceedings of the Conference ISIE'95*, Athens, Greece, 1995.
5. A. L. Nelson and M. Y. Chow, "Electric Vehicles and Axial Flux Permanent Magnet Motor Propulsion Systems," *IEEE Industrial Electronics Society Newsletter: New Technologies*.
6. H. Satoh, S. Akutsu, T. Miyamura, and H. Shinoki, "Development of Traction Motor for Fuel Cell Vehicle," SAE Technical Paper Series (Paper No. 2004-01-0567), reprinted from *Advanced Hybrid Vehicle Powertrains 2004* (SP-1833).